MONTE CARLO SIMULATION OF STEADY-STATE DIFFUSE REFLECTANCE SPECTROSCOPY IN ARTERIAL TISSUES

E. Péry*, L. Bauer*, W.C.P.M. Blondel*, J. Didelon*, ** and F. Guillemin*, **

* Centre de Recherche en Automatique de Nancy
UMR 7039 CNRS – Université Henri Poincaré – Institut National Polytechnique de Lorraine
54516 Vandoeuvre-Lès-Nancy Cédex, France.
** Centre Alexis Vautrin, 54511 Vandoeuvre-Lès-Nancy Cédex, France

emilie.pery@ensem.inpl-nancy.fr

Abstract: Optical methods, such as reflectance and fluorescence spectroscopy, have shown the potential to characterize biological tissues. The goal of the work presented here is to experimentally verify Monte Carlo modeling of steady-state diffuse reflectance measurements between 400 and 800 nm in arterial tissues. Experiments and simulations are carried out with the same parameters (NA of fibers, emission source…). The results indicate that there is good correlation between the simulated and experimentally measured results.

Introduction

The Monte Carlo method has been widely used to simulate light propagation in tissues for nearly two decades [1, 2]. Monte Carlo simulation has been developped to solve various physical problems besides laser-tissue interactions. This type of statistic simulation is well adapted to calculate light transmission and reflectance following absorption and diffusion in complex structures such as the biological tissues and to solve the problems of identification of their optical coefficients.

In our previous studies [3, 4], we used autofluorescence and elastic scattering spectroscopy to show the existence of a correlation between optical spectra and rheological properties (stress – strain characteristics) of artery rings before and after cryopreservation.

The study presented here is to extend the experimental work through a Monte Carlo simulation in order to confirm the spectral behaviour from the known (published) optical properties.

Based on programs already developped in the literature [5, 6], we have implemented a Monte Carlo model of steady-state light transport in arterial tissues with specific features, like multiple distances of reflectance fibers, spectral resolution and the consideration of a whole spectrum by successive samples. Actually, simulations developped in the literature rather use monochromatic light sources than broad band spectrum sources. Considering the whole wavelength range from 400 to 800 nm should allow to better characterize the optical contribution of the different layer consituants.

The final objective of this work in comparing the experimental and theoretical spectra is to be able to determine an index of deformation based on optical parameters.

Materials and Methods

Segments of carotid arteries were harvested from four adult pigs weighing between 20 and 30 kg, following a potassium injection. Each pig carotid artery segment was cut in 4 rings of about 4 mm in length: overall, 16 rings. Diffuse reflectance spectra and mechanical stress were measured for each ring in a water bath, just after excision and after one-month cryopreservation [7] at different elongations [3].

Measurements

An uniaxial mechanical testing device was used for stretching the ring and measuring the elongation and the corresponding axial force. Rings were stretched from 0% to 70% by 10% steps. Circumferential large strains and stresses were calculated.

Simultaneously, an elastic scattering spectroscope was used for recording spatially resolved diffuse reflectance spectra at two distances between illumination and acquisition fibers: 0.53 mm and 1.74 mm between 400 and 800 nm. This device used an USB2000 spectrometer (Ocean Optics, France; pixel resolution≈0.32 nm) connected to a computer and a specifically developed software to collect, process and store elastic scattering spectra for each strain applied.

ISSN: 1727-1983

The light source combined three LEDs covering 400 to 800 nm and a specific seven fiber optic probe (200 μm core diameter) was used for the experiments. The probe was maintained with a specific device and adjusted to come in gentle contact with the upper surface of the arterial tissue during tests.

The mechanical test bed and the spectrometers were calibrated, before each experiment and after every new sample. Before mechanical tests, two different images of each ring were acquired: one, in the unloaded state, served to measure the initial reference dimensions leading to calculate the annular sample volume and the other one served to define the reference length x_0 corresponding to the initial length set on the test bench at measurement start (this picture was taken by slightly squeezing the arterial ring so as the two opposite walls should come into contact with each other).

At the beginning of the tests, the arterial ring was pre-conditionned with a constant deformation of 10 % during three minutes in order to decrease the relaxation phenomena of the sample. In the same way, with each new deformation applied, a relaxation time was left to the sample to release itself before the beginning of the mechano-optical measurements so as to limit the viscoelastic effect.

Modeling

General parameters: The trajectory of the photons is simulated in the 600 nm to 800 nm spectral field and in a semi-infinite medium with three layers corresponding to the adventice, the media and the intima layers of the arterial tissue. The program calculates the energy quantities deposited with each event according to $\mu_a(\lambda)$ and $\mu_s(\lambda)$. Three coordinate systems can be used in the Monte Carlo simulation at the same time. A cartesian coordinate system is used to trace photon movements; a cylindrical coordinate system to score internal photon absorption as a function of r and z, where r and z are, respectively, the radial and z coordinates of the cylindrical coordinate system and finally, a spherical coordinate system to sample of the propagation direction change of a photon.

Each layer is described by the following parameters: the thickness e, the absorption coefficient μ_a (cm^{-1}), the scattering coefficient μ_s (cm^{-1}), the refractive index n, and the anisotropy factor g (see Fig. 1). The refractive indices of the ambient medium above the tissue was air and the ambient medium below the tissue was an isotonic NaCl solution (n=1.33). The tissue layers are parallel to each other.

We determined the experimental values of the various parameters to be used in our model like the respective thickness of the three layers of the arteries according to the histological cuts realized and images of each ring.

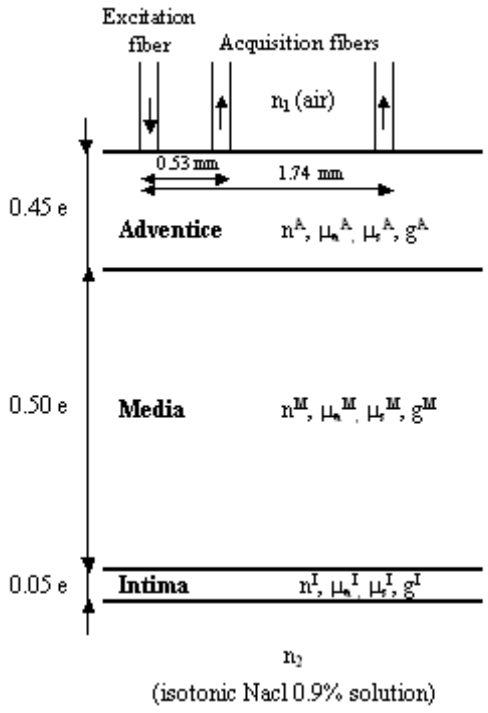

Figure 1: Schematic representation of the three-layers model used to simulate light transport in an arterial tissue. e is the total thickness; n^i, μ_a^i, μ_s^i, g^i are respectively the refractive index, the absorption coefficient, the scattering coefficient, and the anisotropy factor for the adventice (i=A), the media (i=M) and the intima (i=I).

The numerical values used in our simulation for the optical parameters of the intima, the media, the adventice (Table 1) and the refractive indices (Table 2) for arterial tissue were chosen from the literature [8, 9].

Table 1: Values of optical parameters for arterial tissue chosen from the literature and implemented in our simulation program.

Description	Wavelength (nm)	μ_a (cm^{-1})	μ_s (cm^{-1})	g	Ref
Intima	476	14.8	237	0.81	8
	580	8.9	183	0.81	8
	600	4	178	0.81	8
	633	3.6	171	0.85	8
	1064	2.3	165	0.97	9
Media	476	7.3	410	0.89	8
	580	4.8	331	0.9	8
	600	2.5	323	0.89	8
	633	2.3	310	0.9	8
	1064	1	634	0.96	9
Adventice	476	18.1	267	0.74	8
	580	11.3	217	0.77	8
	600	6.1	211	0.78	8
	633	5.8	195	0.81	8
	1064	2	484	0.97	9

ISSN: 1727-1983

Table 2: Values of the refractive index for arterial tissue.

Description	Wavelength (nm)	*n*	Ref
Intima	456-1064	1.39	9
Media	456-1064	1.38	9
Adventice	456-1064	1.36	9

In order to work in a broad-band spectrum (between 600 and 800 nm), we have interpolated the five values found in the literature to find the values corresponding to the other wavelength (20 values), one value each 10 nm. Ten million photons were launched in each simulation at random uniformly distributed locations, i. e. ten millions photons for 20 wavelengths values.

Configuration parameters of the program include illumination and collection fiber geometries, three-dimensional light distribution in tissues multiple layers, wavelength resolution.

Simulating photon propagation: Step 1, the photon is injected orthogonally into the tissue at the origin, which corresponds to a collimated infinitely narrow beam of photons. The photons emitted by the source (parameters corresponding to the light source used in our experiments) are launched with a random trajectory and are included in the surface of the emission fiber. When the photon is launched, if there is a refractive-index-mismatched interface between the tissue and the ambient medium, some specular reflectance will occur. If the refractive indices of the outside medium and tissues are n_1 and n_2 respectively, then the specular reflectance, R_{sp}, is expressed by the relation [10]:

$$R_{sp}=\frac{(n_1-n_2)^2}{(n_1+n_2)^2} \qquad (1)$$

Step 2, if photons hit an interface between two layers (all-or-none method), either they are completely refracted ($n_i < n_t$ where n_i and n_t are the refractive indices of the incident and transmitted layers), or they are completely reflected ($n_i > n_t$ and $a_t > a_c$ where a_t corresponds to the angle of transmission and a_c the critical angle), or the two cases are possible ($n_i > n_t$ and $a_t < a_c$) according to the reflective coefficient. This reflective coefficient, $R(a_i)$, is calculated by Fresnel's formulas [10]:

$$R(a_i)=\frac{1}{2}\left[\frac{\sin^2(a_i-a_t)}{\sin^2(a_i+a_t)}+\frac{\tan^2(a_i-a_t)}{\tan^2(a_i+a_t)}\right] \qquad (2)$$

where a_i is the angle of incidence.

With each stage, the energy deposited with each event is recorded and cumulated for all photons.

Step 3, photons can terminate in three differents ways. After a photon travels, it can be counted out of the tissue by reflection or transmission. Through diffuse reflexion, some photons can be collected in the diffuse reception fibers. Finally, when the energy left for a photon is less than a threshold value, a chance of surviving is given following the Russian roulette technique [11].

Results and Discussion

Experimental results: A typical example of the elastic scattering spectra collected at both distances (channel 1: 0.53 mm and channel 2: 1.74 mm) is presented in Fig. 2 for three different strains imposed on the same sample (ring n°13).

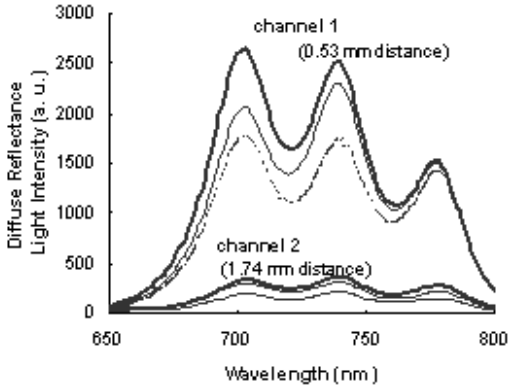

Figure 2: Typical example of elastic scattering spectra of an artery ring (n°13) for strains of 0% (full line), 30% (fine line) and 60% (dotted line) at 0.53 mm (channel 1) and 1.74 mm (channel 2) excitation-emission distances.

These results show us that the global intensity of spectra decreases as strains rise. These variations are less marked for channel 2 than for channel 1. The longer course, that the photons must carry out between excitation fibers of the channel 2 and the reception fiber, seems to correspond to a stronger absorption by the arterial tissue, which results in a lower total intensity second group of spectra (channel 2).

Looking at the graphics in Fig. 2 for channel 1 (0.53 mm emission distance), we observe a significant diminution of the diffuse reflectance light intensity.

ISSN: 1727-1983

The spectra resulting from scattered photons coming from the excitation channel 1 thus seem to be good indicators of the differences in optical behavior and in mechanical state of deformation of the samples tested. Elastic scattering spectra intensity variations are well correlated with structure organization modifications due to elongation, thus with artery mechanical properties.

On the contrary, we notice that the light intensity corresponding to the diffused photons issued from channel 2 (1.74 mm emission distance) only varies very little with strains.

Simulation results: We obtain the spatial distribution, i. e. the fluence according to the radial distance and we recover the spectra of intensity and diffusion. The diffuse reflectance spectra simulated are shown in Fig. 3 for artery ring n°13.

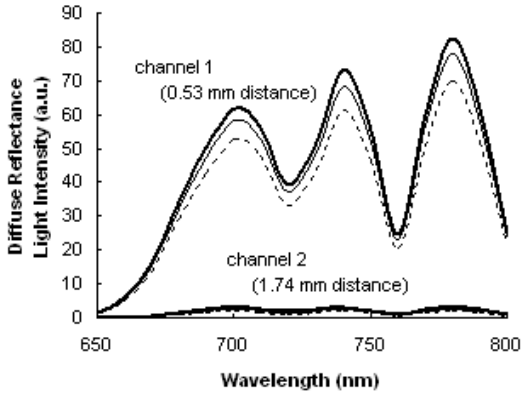

Figure 3: Corresponding simulation results (artery ring n°13) of diffuse reflectance for strains of 0% (full line), 30% (fine line) and 60% (dotted line) at 0.53 mm (channel 1) and 1.74 mm (channel 2) excitation-reception distances.

We can notice that for the experiments and for the simulation, the global intensity of spectra decreases as strains rise and these variations are less marked for channel 2 than for channel 1. However, a more important level of diffuse reflectance light intensity can be observed in simulation in the red wavelength range.

By looking more precisely the optical parameters, especially μ_s and in particular the values at 1064 nm, we can observe that μ_s decreases between 400 nm and 633 nm before increasing considerably at 1024 nm. Our interpolation between 633 nm and 800 nm takes account of this last value at 1064 nm. It could affect our simulation results.

Furthermore, the more important level of diffuse reflectance light intensity in the red wavelength range can be explained by the course of the photons.

As the μ_s value at 1064 nm (for the adventice and for the media) is higher than the μ_s value at 633 nm, the diffusion distance is larger for weaker absorptions (see Table 1: at 1064 nm, μ_s=634 cm^{-1} and μ_a=1 cm^{-1} for the adventice); the collected diffuse reflectance light intensity is bigger.

If the μ_s value at 1064 nm is weaker than the μ_s value at 633 nm, the events of absorption are more numerous because the length of diffusion is shorter. So, the diffuse reflectance light intensity found in the red wavelength range would be smaller.

In order to precise possible correlation between the spectral variations and the strain value variations, we calculate the area under the curve for each spectrum, for each imposed strain and for each channel. Results are plotted in Fig. 3.

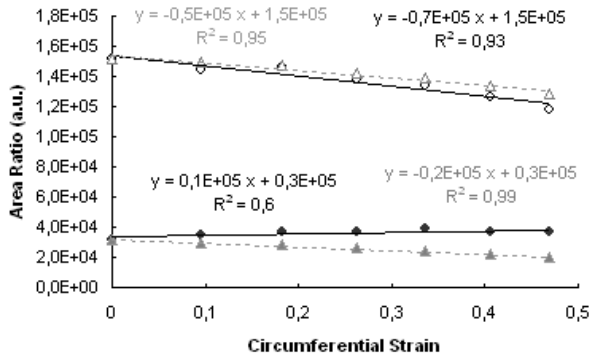

Figure 3: Diffuse reflectance intensity spectrum area under the curves for the average of all the samples.
The round and points correspond respectively to the experimental and the simulation. Empty and full points correspond to measurements performed at 0.53 mm (channel 1) and 1.74 mm (channel 2) excitation – reception distances.

Looking at the graphics in Fig. 3 for channel 1 (0.53 mm emission distance), we observe a significant diminution of the integrated spectral intensities. We can see that the curves have the same behaviour, especially for the channel 1.

The used theorical model seems to simulate correctly the observed behaviour in experiments.

ISSN: 1727-1983

Conclusions

The results obtained with simulation through a three-layer model confirm the correlation between the optical property variations and arterial tissue ring deformation.

Our simulation program takes into account absorption and diffusion of light over a broad band spectrum.

It will be interesting to continue this work with a validatation of this model in other tissues, with an implementation of the fluorescence in the simulation program and to work in the identification of the optical parameters.

Acknowledgements

The Authors gratefully acknowledge the "Région Lorraine" and the "Ligue Contre Le Cancer (CD54)" for their financial support.

References

[1] METROPOLIS, N., AND ULAM, S. (1949): 'The Monte Carlo method', J. Am. Statistical Association., **44**, pp. 335-341

[2] WILSON, B.C., AND ADAM, G. (1983): 'A Monte Carlo model for the absorption and flux distribution of light in tissue', Med. Phys., **10**, pp. 824-830

[3] CHOSEROT, C., PÉRY, E., GOEBEL, J.C., DUMAS, D., DIDELON, J., STOLTZ, J.F., AND BLONDEL, W.C.P.M. (2005): 'Experimental Comparison between Autofluorescence Spectra of constrained Fresh and Cryopreserved Arteries', Clin. Hemorheol. Microcirc., in press

[4] PÉRY, E., GOEBEL, J.C., BLONDEL, W.C.P.M., DIDELON, J., AND GUILLEMIN, F. (2005): 'Spectral (optical) and mechanical responses of fresh and cryopreserved issued arteries', Proc. of SPIE, **5695**, pp. 66-74

[5] PRAHL, S.A., KEIJZER, M., JACQUES, S.L., AND WELCH, A.J. (1989): 'A Monte Carlo Model of Light Propagation in Tissue', Proc. of SPIE, **IS 5**, pp. 102-111

[6] WANG, L., JACQUES, S.L., AND ZHENG, L. (1995): 'MCML – Monte Carlo modelling of light transport in multi-layered tissues', Computer Methods and Programs in Biomedicine, **47**, pp. 131-146

[7] ROSSE, E., FRIGGI, A., NOVAKOVITCH, G., ROLLAND, P.H., RIEU, R., PELLISSIER, J.F., MAGNAN, P.E., AND BRANCHEREAU, A. (1996): 'Effects of cryopreservation on the viscoelastic properties of human arteries', Ann. Chir. Vasc., **10 (3)**, pp. 262-272

[8] CHEONG, W.F., PRAHL, S.A., AND WELCH, A.J. (1990): 'A Review of the Optical Properties of Biological Tissues', IEEE J. Quantum Electron., **26**, pp. 2166-2185

[9] MULLER, G., AND ROGGAN, A. (1995): 'Laser-Induced Interstitial Thermotherapy', Proc. of SPIE, **PM25**, Bellingham, WA

[10] BORN, M., AND WOLF, E. (1986): 'Principles of Optics: Electromagnetic Theory of Propagation', Interference and Diffraction of Light, 6th edition, Pergamon Press

[11] HENDRICKS, J.S., AND BOOTH, T.E. (1985): 'MCNP variance reduction overview', Lect. Notes Phys., **240**, pp. 83-92

ISSN: 1727-1983